STUDY FOR REYNOLDS NUMBER EFFECT ON C_{lmax} OF 2-DIMENSIONAL AIRFOILS

Kenji YOSHIDA and Hirokage OGOSHI
Gifu Technical Institute , KAWASAKI HEAVY INDUSTRIES , LTD.
1. Kawasaki-cho , kakamigahara City , Gifu , 504 , Japan

Abstract

The behavior of the C_{lmax} of 2-dimensional airfoils at a high Reynolds numbers was investigated numerically and experimentally . In the present study , the so-called "adverse effect" which means the decrease of the C_{lmax} at a high Reynolds number is mainly considered . Firstly the Reynolds number effect of a transition point on several NACA 4-digit series airfoils was analyzed , using a potential flow theory and boundary layer theory with an empirical transition prediction method . Secondly a criterion on the possibility of the occurrence of the adverse effect was developed , based on the correspondence between those numerical results and experimental results on C_{lmax} by NACA . Finally wind tunnel tests on the following airfoils were conducted to validate our criterion : They are three typical airfoils named NACA 8318 , 6212 and 4412 respectively , which correspond to three kinds of the possibility of the occurrence of the adverse effect as follows : 100% , 50% and 0% . And confirming the adverse effect on an NACA 6212 airfoil , it was found that our criterion was useful to judge whether such adverse effect occurred or not .

1. Introduction

In the aerodynamic design of an aircraft , it is very important to estimate the characteristics at high Reynolds numbers , based on the results obtained by wind tunnel tests . Especially the behavior of C_{Lmax} at high Reynolds numbers plays a major role in landing . Generally it is expected that as the Reynolds Number increases , the C_{Lmax} also increases . Recently using a pressurized wind tunnel , however , the decreases of the C_{Lmax} at a high Reynolds number on some typical swept wings were observed.[1][2] This is called the "adverse effect" for a Reynolds number .

Moreover it is generally known that such adverse effect is also observed in wind tunnel tests on some typical 2-dimensional airfoils , such as NACA 8318 and 9324.[3][4] Presently it is qualitatively understood that the mechanism of this phenomenon is based on the forward movement of a transition point.[5] But it is difficult to predict the Reynolds number effect of the C_{lmax} quantitatively .

Therefore more detailed investigations of the Reynolds number effect on the maximum lift of both two and three dimensional wings are desired . As a first step for such studies , we investigated the behavior of the C_{lmax} of 2-dimensional airfoils numerically and experimentally . The purpose of the present study is to understand the mechanism of the adverse effect in detail and to develop a method predicting the behavior of the C_{lmax} at high Reynolds numbers .

First of all , using a potential flow theory and boundary layer theory with an empirical transition prediction method , the relation between a transition position and a Reynolds number on a lot of NACA 4-digit series airfoils was analyzed . Then according to the correspondence between our numerical results and experimental results on C_{lmax} obtained by NACA , a criterion on the adverse effect was made .

Next wind tunnel tests on the following three typical airfoils were conducted : They are an

NACA 8318 , 6212 and 4412 airfoil , which correspond to three kinds of the possibility of the occurrence of the adverse effect as follows : 100% , 50% and 0% respectively . And confirming the adverse effect on an NACA 6212 airfoil , it was found that our criterion was useful to judge the occurrence of the adverse effect .

In the present paper , first of all , a brief explanation about the mechanism of the adverse effect on both a simple swept tapered wing and a two-dimensional airfoil is given in section 2 as a background . Next the results of our numerical and experimental studies are mentioned in section 3 and 4 respectively . And finally a criterion on the adverse effect is presented in section 5 as a summary in our study .

2. Background

2.1 The behavior of C_{Lmax} of 3-dimensional wings

First of all , we show two wind tunnel results on the adverse effect of 3-dimensional wings in Fig.1 and 2.[1][2] The abscissa and ordinate of Fig.1 denote an unit Reynolds number and a ratio of the C_{Lmax} to the maximum value in the range of a test Reynolds number . Generally as the Reynolds number increases , the spanwise position of the transition caused by the so-called attachment-line contamination moves from the tip region to the root . When the spanwise position of the transition exists below about 82 % semi-span length ($\eta <$ 0.82) , the decrease of the C_{Lmax} is seen in Fig.1 .

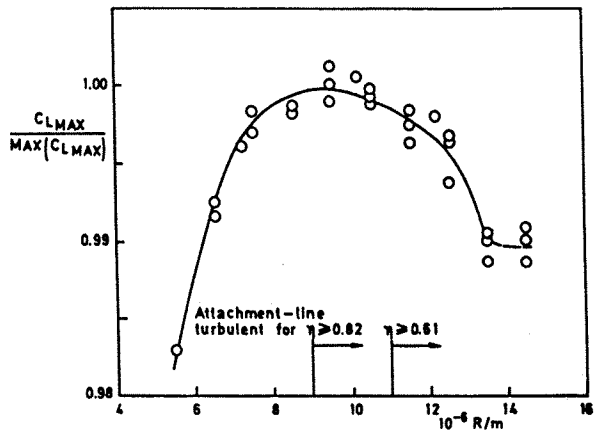

Fig.1 Adverse effect on C_{Lmax} by RAE[1]

And the influence of leading edge shape on the onset Reynolds number where the adverse effect occurs is shown in Fig.2 . And it is observed that the onset Reynolds number decreases in a 3-dimensional wing with a larger leading edge radius . This is based on the following fact : In the case of a simple swept wing with a larger leading edge radius , it is estimated that the transition due to the attachment-line contamination occurs at a lower Reynolds number , according to the well-known Poll's criterion.[1]

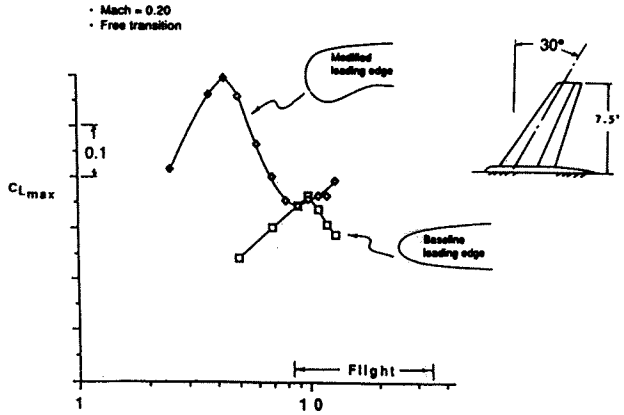

Fig.2 Adverse effect on C_{Lmax} by Boeing[2]

Ref.1 presently gives an aerodynamic explanation about the mechanism of such adverse effect as follows : In a simple swept wing , the transition due to the attachment-line contamination near the leading edge occurs at a high Reynolds number . This means that the turbulent boundary layer on the upper surface grows from the stagnation point . Generally it is pointed out that the C_{lmax} of a 2-dimensional airfoil decreases when the boundary layer from the stagnation point fully becomes turbulent.[1]

By the way , in the case of a simple swept wing , the spanwise position where the local C_l becomes maximum , usually exists in the region of about 70 ~80% semi-span . And if that local maximum C_l decreases , the total C_L also decreases , and this leads to the decrease of the C_{Lmax} .

Certainly this phenomenon depends on the wing geometry . Especially the leading edge radius is very important . And as mentioned

above , according to the Poll's criterion , wings with a larger radius cause such transition at a lower Reynolds number , therefore they have a high possibility on the occurrence of the adverse effect . On the other hand , if the leading edge radius is smaller , however , the so-called re-laminarization for the turbulent boundary layer is caused by a strong accelerated flow near the leading edge . Consequently no adverse effect occurs at that Reynolds number . The difference of the onset Reynolds number on the adverse effect seen in Fig.2 is qualitatively explained by this mechanism .

But Ref.1 has never given any quantitative criterion on the occurrence of the adverse effect and method predicting the characteristics at high Reynolds numbers . So it is desired to make such a criterion and a method in the viewpoint of the high Reynolds number correction .

2.2 The behavior of C_{lmax} of 2-dimensional airfoils

Some typical wind tunnel results[3] on the C_{lmax} of NACA airfoils are summarized in Fig. 3 . It is seen in this figure that the C_{lmax} of an NACA 8318 decreases with the increase of the Reynolds number , as compared with the increase of the C_{lmax} of other airfoils .

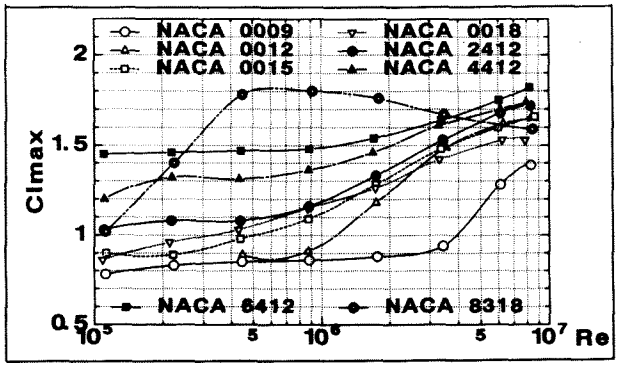

Fig.3 Variation of C_{lmax} with Reynolds number by NACA[3]

Generally the physical mechanism of this phenomenon is different from the mechanism on a 3-dimensional wing . According to Ref.5 , the Reynolds number effect on the behavior of the C_{lmax} of a 2-dimensional airfoil is schematically summarized in Fig.4 and it is explained as follows :

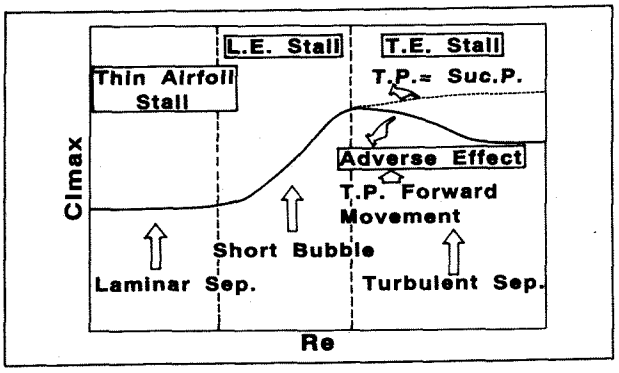

Fig.4 Mechanism of adverse effect by Tani[5]

First of all , in the region of low Reynolds numbers , the C_{lmax} is mainly dominated by laminar separation , and it is independent of a Reynolds number according to the boundary layer theory . Therefore the C_{lmax} is considered to be nearly constant for the Reynolds number .

Next as a Reynolds number increases , the laminar separated flow reattaches on the surface and the so-called laminar separation bubble is formed . Therefore the angle of attack to keep an attached flow near the leading edge increases , then the C_{lmax} slightly increases .

And as the Reynolds number increases furthermore , natural transition is caused before the laminar separation occurs . In usual airfoils which don't have a large camber and thickness , the transition point is almost coincident with the position of suction peak on a pressure distribution at a high angle of attack . Generally the increase of a Reynolds number reduces the thickness of turbulent boundary layer . Therefore the reduction of a circulation around an airfoil due to viscous effect is relaxed . Consequently the C_{lmax} slightly increases .

On the other hand , in some airfoils such as an NACA 8318 airfoil which has a larger camber and thickness than usual airfoils , the adverse pressure gradient after the suction peak point is not strong even at a high angle of attack . So the natural transition is located fairly downstream from the suction peak point . In this situation , if

the Reynolds number increases , the transition point moves forward to the suction peak point . Consequently the turbulent boundary layer on the upper surface is thickened . Therefore the circulation is reduced , and this effect leads to the decrease of the C_{lmax} .

Though the above explanation was already given by Professor Tani a half century ago , thereafter there were few studies on such characteristics of C_{lmax} . About 15 years ago , however , Kamiya et al.[4] studied the same subject according to Tani's suggestion . And they pointed out that the behavior of C_{lmax} for various Reynolds numbers corresponded to the inverse behavior of the C_d of a circular cylinder , and found that an NACA 9324 airfoil also showed the adverse effect . Further by using a technique of distributed roughness reducing the transition Reynolds number , they tried to simulate a high Reynolds number condition at a low Reynolds number test and estimated the behavior of the C_{lmax} of an NACA 9324 airfoil . A criterion on the relation between the adverse effect and airfoil geometry , however , has not been made clear yet .

3. Numerical Study

3.1 Method of analysis

Presently there is no method predicting the Clmax of a 2-dimensional airfoil quantitatively , in spite of great advances in CFD . Therefore we paid attention to the qualitative relations of airfoil geometry , suction peak , laminar separation and transition at various Reynolds numbers .

In this numerical study , a method based on a potential flow theory[6] was used , in order to predict pressure distributions around an airfoil . And a method by Thwaite[7] in analyzing the characteristics of a laminar boundary layer , and an empirical method by Michel[8] in predicting a transition point were used . Further NACA 4-digit series airfoils were chosen . Because their geometry's are calculated analytically and characterized by the following three parameters : a maximum camber (f/c) , a maximum camber position (x_m/c) and a thickness to chord ratio (t/c) .

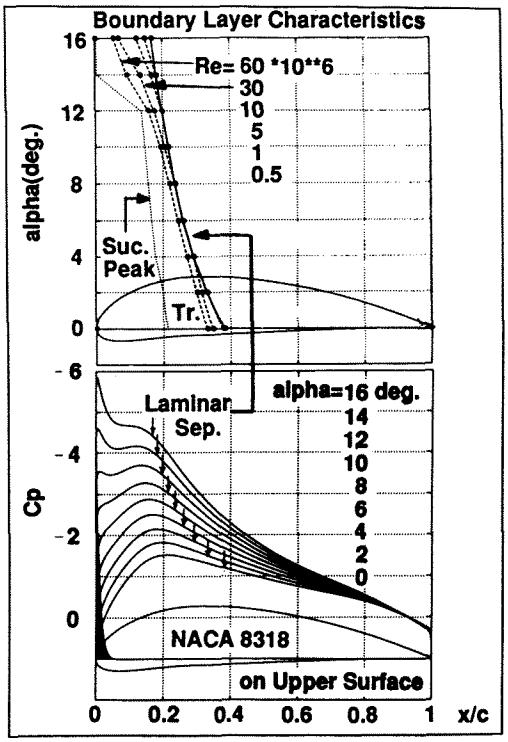

Fig.5 Numerical analysis on NACA 8313

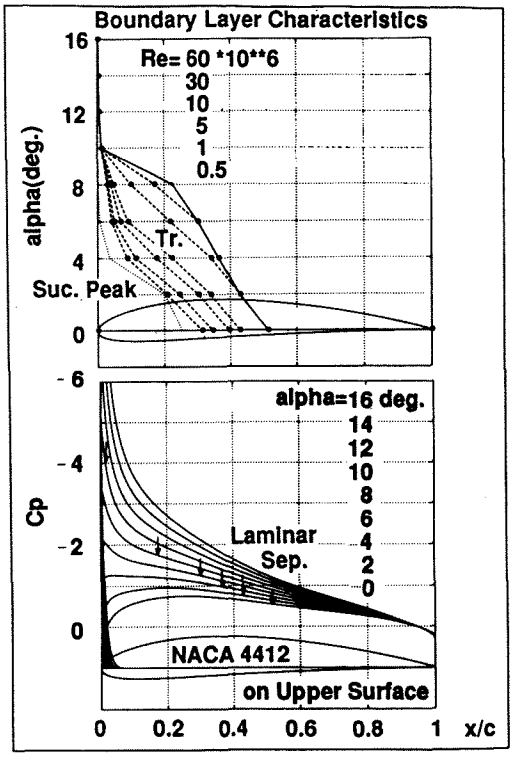

Fig.6 Numerical analysis on NACA 4412

First of all , we analyzed an NACA 8318 airfoil and summarized the results in Fig.5 . It is seen that the laminar separation point is located fairly

downstream from the suction peak point even at a high angle of attack , such as 16° . And it is obtained that the natural transition moves forward as the Reynolds number increases .

Next as a representative airfoil which is experimentally confirmed to indicate no adverse effect , the results on an NACA 4412 airfoil are summarized in Fig.6 . At a high angle of attack , the laminar separation point nearly coincides with the suction peak point , and the forward movement of the transition point is not seen .

These qualitative features agree fairly well with Tani's explanation . Therefore we considered that we could make a criterion on the occurrence of the adverse effect , by summarizing the correspondence of present qualitative analysis to experimental results by NACA and Kamiya et al. .

3.2 Parametric Study

As the second step , we carried out those analysis on various NACA 4-digit series airfoils shown in Fig.7 . Consequently it was found that the behavior of a suction peak point , a laminar separation point and a transition point on various Reynolds numbers was divided into several patterns as summarized in Fig.8 . These patterns schematically show the upper part of Fig.5 and 6 .

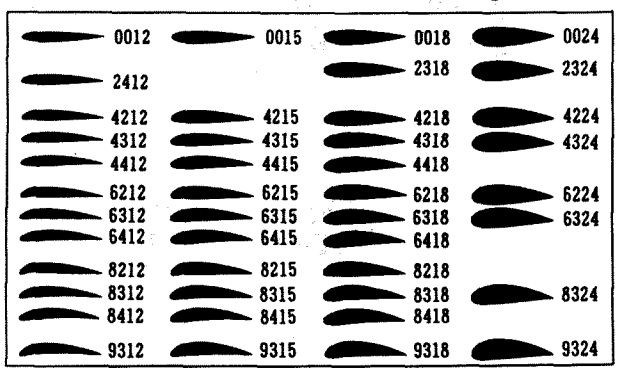

Fig.7 NACA 4-digit series airfoils for present numerical study

First of all , as the "Type A" corresponds to the pattern on NACA 8318 , it is estimated that airfoils with this "Type A" pattern "almost" show the adverse effect . In this figure , these airfoils are indicated by the symbol of a closed circle (●) .

Next the "Type B, C, D, E" patterns show that there is a large distance between the suction peak point and the laminar separation point . Therefore since they have a possibility of the forward movement of a transition point , it is estimated that they "probably" show the adverse effect . But as the amount of that movement is shorter than the "Type A" , it is also considered that they don't always show the adverse effect . Therefore airfoils with these patterns are indicated by the symbol of a half open and closed circle (◐) .

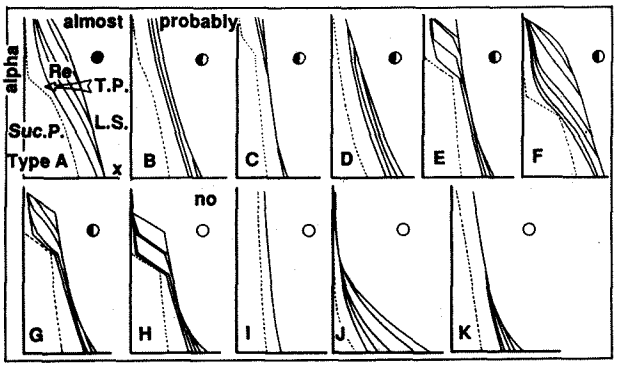

Fig.8 Several patterns on the relation between laminar separation and transition

And since the "Type F, G" patterns also show that there is a large distance . It is generally estimated that airfoils with these patterns "probably" show the adverse effect . But the distance rapidly disappears at a certain high angle of attack . If these airfoils have the C_{lmax} above that high angle of attack , it is considered that they don't show the adverse effect . Therefore these patterns are also indicated by the symbol of a half open and closed circle (◐) .

On the other hand , as the "Type H, I, J" patterns show that there is no distance at a high angle of attack , it is estimated that they have "no" possibility of the occurrence of the adverse effect . And as the "Type K" shows that there is no forward movement of a transition point at a high angle of attack in spite of a large distance , it is also considered to show "no" adverse effect . Therefore these patterns are indicated by the symbol of a open circle (○) .

According to the above consideration , we

summarized the possibility of the occurrence of the adverse effect on NACA 4-digit series airfoils in Fig.9 . Generally a potential flow theory easily derives the relations between three representative parameters (f/c,x_m/c,t/c) and pressure distributions as follows :

The increase of a maximum camber (f/c) , the forward movement of a maximum camber position (x_m/c) and the increase of a thickness ratio (t/c) similarly lead to the increase of a leading edge radius . And this leads to the decrease of local velocity at the suction peak point and the relaxation of adverse pressure gradient downstream from that point . Consequently the laminar separation point moves downstream , and a large distance between the suction peak point and the laminar separation point is generated . Therefore it is considered that the above conditions mean the high possibility of the occurrence of the adverse effect . The result of Fig.9 seems to correspond to this trend .

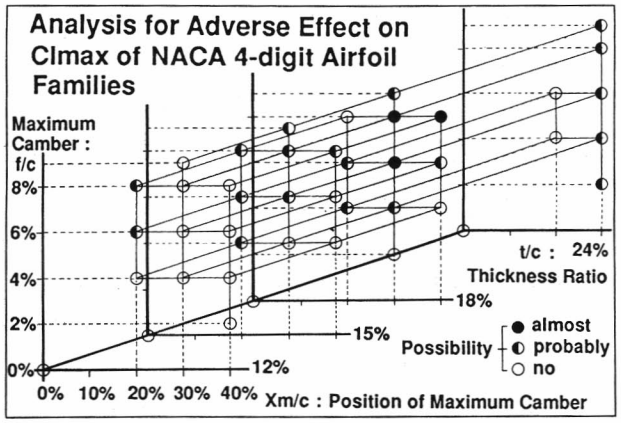

Fig.9 A criterion for adverse effect

In the present study , our purpose is to develop a criterion on the occurrence of the adverse effect . In order to try it based on Fig.9 , it is necessary to confirm whether airfoils indicated by a half open and closed symbol (◐) show the adverse effect or not . Therefore as the next study , we carried out wind tunnel tests on the following airfoils : NACA 8318 , 4412 and 6212 . The former two airfoils were chosen to confirm the experiments by NACA . And the last one was chosen as a trial airfoil to investigate the present question .

4. Experimental Study

4.1 Outline of present wind tunnel test

As a technique to realize a 2-dimensional flow condition in our test , a straight wing with large end-plates at both tips shown in Fig.10 was used . And pressure distributions at the center of the span and total forces by a force balance were measured . Wind tunnel test models are shown in Fig.11 . The test facility is a low speed wind tunnel with a test section size of 2.5 m × 2.5 m at Kawasaki Heavy Industries . The range of the test Reynolds number based on a chord length is from about 0.2 to 1.1 million corresponding to the free stream velocity from 10 to 60 m/s .

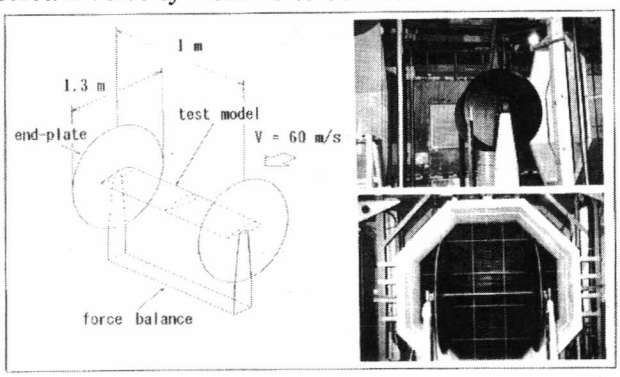

Fig.10 Wind tunnel test setup

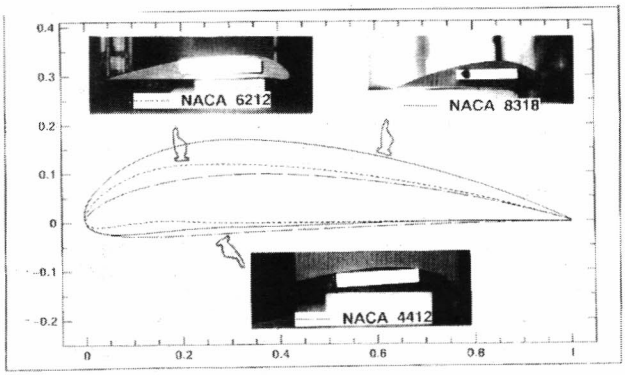

Fig.11 Test models

By the way , we are also interested in the behavior of the C_{lmax} at higher Reynolds numbers . So in the present test , we tried to simulate a high Reynolds number condition by distributed roughness . Generally the distributed roughness on the surface amplifies small disturbances in the boundary layer and causes early transition .

Therefore it is considered that this corresponds to the higher Reynolds number condition .

The roughness which we used consists of a thin film with lots of micron-sized particles , and it was put on the surface from 20% chord position at the lower surface to 70% at the upper surface shown in Fig.12 . The parameter is the height of a particle mounted on the film and two films with the height of 30 and 60 μ m were chosen .

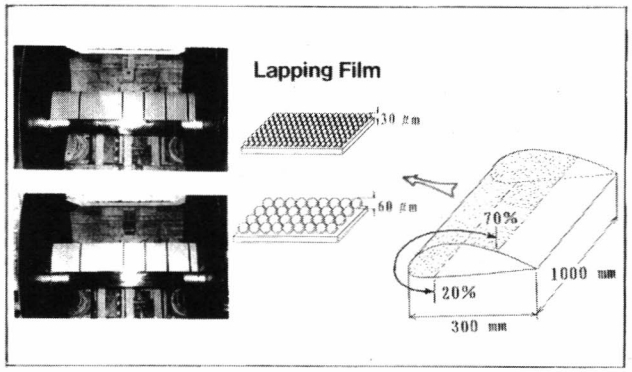

Fig.12 Distributed roughness

4.2 Characteristics of C_{lmax}

4.2.1 Case of smooth surface

First of all , the comparison of the C_l integrated through a pressure distribution and measured by a force balance was investigated at the test Reynolds number of 0.75 million on NACA 8318 . As seen in Fig.13 , the measured C_l (O) is fairly higher than the integrated C_l (●) , and there are remarkable differences in the C_{lmax} and stall angle . The reason of these differences is considered as follows :

The former depends on the influence of the equipment supporting the model . And the latter depends on three dimensionality as seen in the case of α=20.4° at the lower part of Fig.13 , where y/b shows the spanwise position . Therefore the integrated C_{lmax} doesn't correspond to the true C_{lmax} as a 2-dimensional airfoil . Then we assumed that the integrated C_{lmax} was approximately the C_l at the angle of attack corresponding to the upper limit of keeping two dimensionality of flow .

According to this assumption , the behaviors of the C_{lmax} of an NACA 8318 , 4412 and 6212 airfoil obtained by present test are summarized in Fig.14 and 15 , compared with results of Fig.3 by NACA .

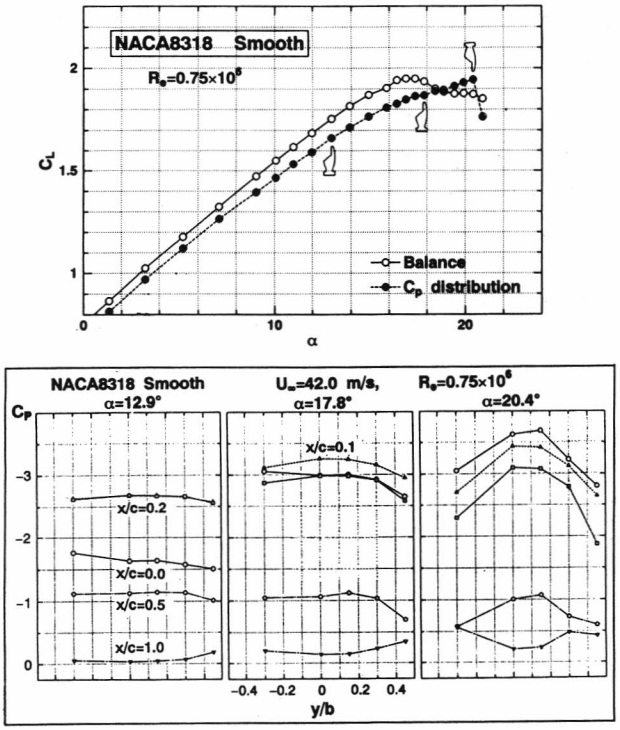

Fig.13 Measured lift curve and spanwise pressure distributions of NACA 8318

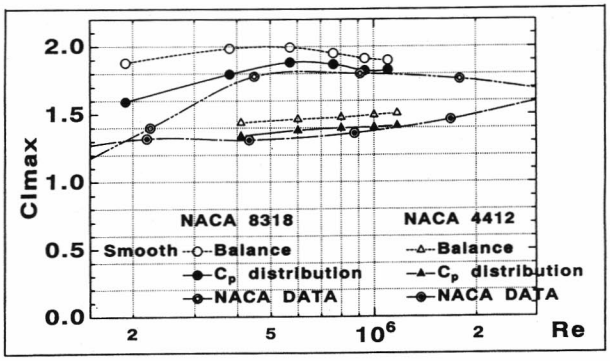

Fig.14 Test results for variation of C_{lmax} with Reynolds number on NACA 8318 and 4412

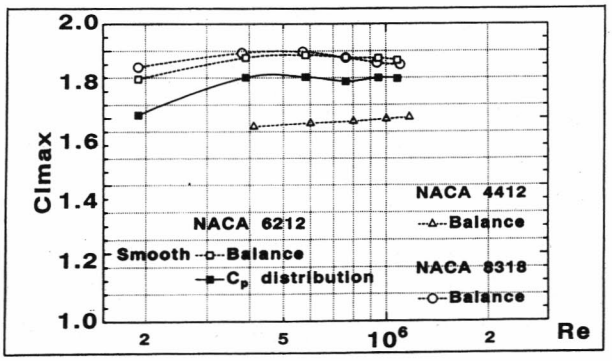

Fig.15 Test results for variation of C_{lmax} with Reynolds number on NACA 6212

And it was observed that there were good qualitative agreements between the measured C_l and the integrated C_l in both figures , and also between the results of our test and NACA in Fig.14 . Consequently we could experimentally confirm the occurrence of the adverse effect on both NACA 8318 and 6212 , and no adverse effect on NACA 4412 .

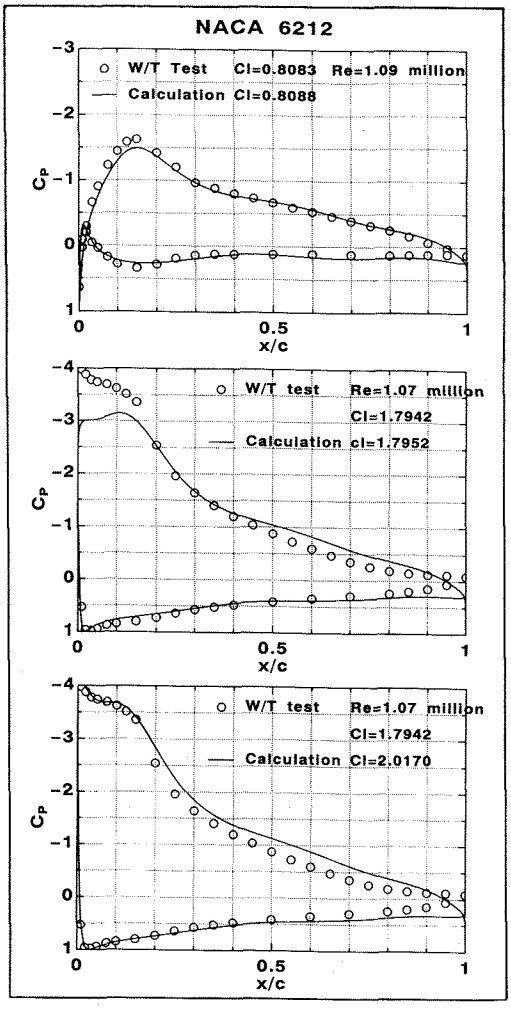

Fig.16 Comparison of measured and calculated pressure distirbutions on NACA 6212

For reference , the comparisons of pressure distributions on NACA 6212 measured and predicted by a potential theory at the same C_l condition are summarized in Fig.16 . In the case of no large turbulent separation , it is seen at the upper part of Fig.16 that there is good agreement on both results . As the C_l increases , however , the difference of them becomes larger , especially the pressure distribution at the front part is different .

But since the attached flow is generally realized at the front part in spite of turbulent separation at the rear part , it is expected that the front pressure distribution can be estimated by a potential flow theory . So we tried to calculate a pressure distribution at the condition of increasing the angle of attack . Consequently it was found that there was good agreement between the front pressure distributions measured and predicted at a larger angle of attack . This means that the present analysis which consists of a potential flow theory and boundary layer theory is effective in investigating the behavior of suction peak , laminar separation and transition .

4.2.2 Case of rough surface

The results of roughness test on NACA 4412 and 6212 are summarized in Fig. 17 and 18 . For simplicity , we only consider the C_{lmax} measured by a force balance , because of qualitative agreement between the measured and the integrated C_{lmax} .

First of all , it was observed in Fig.17 that the C_{lmax} of an NACA 4412 airfoil with the distributed roughness of 60 μ m decreased as the Reynolds number increased . Since an NACA 4412 airfoil originally shows no adverse effect , it is considered that this trend doesn't correspond to the high Reynolds number state and the flow is greatly influenced by the roughness . Therefore this 60 μ m roughness is invalid .

On the other hand , in the case of 30 μ m , the C_{lmax} slightly increases with the increase of the Reynolds number . This behavior is considered to be aerodynamically reasonable , according to Tani's explanation . Therefore this 30 μ m roughness is valid in simulating the high Reynolds number state .

Next as seen from the result of the 30 μ m roughness in Fig.18 . it is estimated that the C_{lmax} of an NACA 6212 airfoil is nearly constant at a

higher Reynolds number . Since it is generally supposed that the forward movement of transition point stops near the suction peak point at a higher Reynolds number , the decrease of the C_{lmax} is suppressed . Therefore this experimental result is considered to correspond to the behavior at high Reynolds numbers .

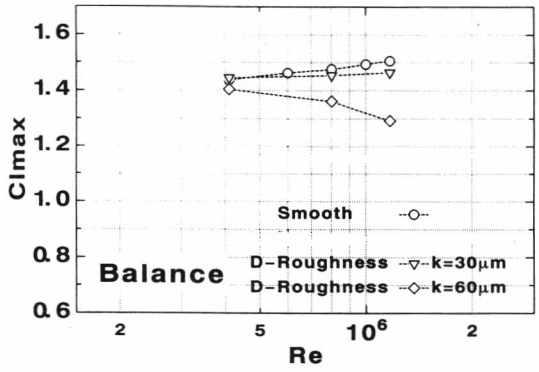

Fig.17 Roughness test results for variation of C_{lmax} with Reynolds number on NACA 4412

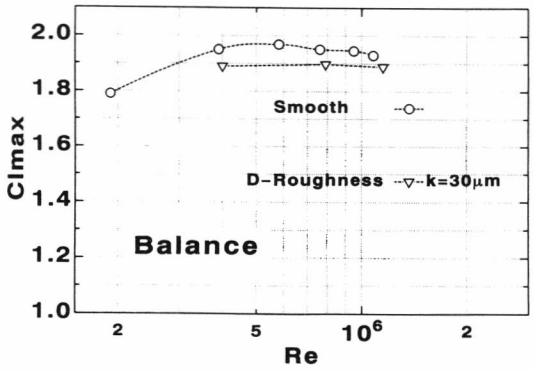

Fig.18 Roughness test results for variation of C_{lmax} with Reynolds number on NACA 6212

4.3 Consideration of forward movement of transition point

The forward movement of a transition point plays the most important role in the occurrence of the adverse effect . At the first wind tunnel test of measuring the C_{lmax} , it was not confirmed . So to make our aerodynamic understanding of the adverse effect clear , we tried to investigate the movement of a transition point experimentally , applying the flow visualization technique of a liquid crystal film .

One of test results on NACA 8318 is shown in Fig.19 . In this figure , the upstream side is left . And three different liquid crystal films with the reference temperature of 14° , 18° and 22° C when colors come out , are put on the left side , middle side and right side of the test wing , respectively . But in this test condition , it was seen that the liquid crystal film with the reference temperature of 18° C was the most suitable . Further , in order to judge whether the change of color means transition or not , the so-called "turbulent wedge" caused by a tiny roughness on the leading edge was used .

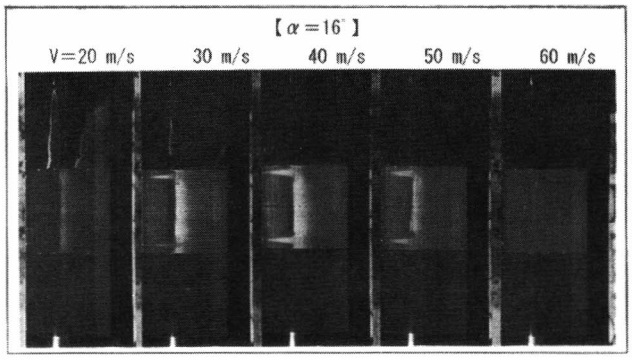

Fig.19 Flow visualization results on NACA 8318

According to these visualization results , the behavior of a transition point is summarized in Fig.20 . The ordinate denotes the position of transition or laminar separation , and the abscissa shows a test velocity related to a Reynolds number . And the symbol of a circle means the stall angle of attack . In this figure , it was certainly seen that the transition point at the C_{lmax} moves forward at a high Reynolds number .

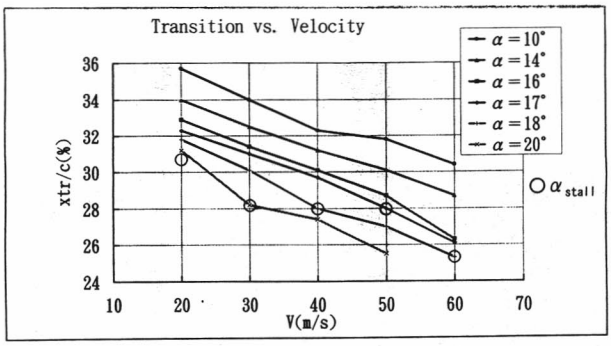

Fig.20 Summary of flow visualization results on NACA 8318 : Transition point vs. Velocity

Also Fig.21 shows the summary of visualization test . And it is seen that there are two trends

indicated by two interpolated lines at a high angle of attack without V=20 m/s . First of all , since the case of V=20 m/s means the low Reynolds number condition , the chain-line is considered to correspond to the laminar separation .

Next at other velocity conditions , as the chain-lines in the range of lower angles of attack are nearly parallel to the chin-line at the case of V=20 m/s , they also correspond to the laminar separation . On the other hand , since the broken-lines in the range of higher angles of attack are not parallel to the chain-lines and since they become longer at higher Reynolds numbers , they seem to mean the transition . In this figure , it is also seen that a transition point at the C_{lmax} indicated by a circle moves forward at a higher Reynolds number .

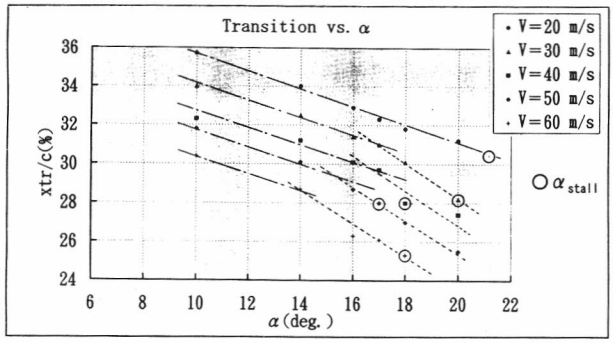

Fig.21 Summary of flow visualization results on NACA 8318 : Transition point vs. α

For reference , results of the visualization test on NACA 4412 are summarized in Fig.22 and 23 . The forward movement is hardly seen in Fig.23 . And this result agrees with our understanding .

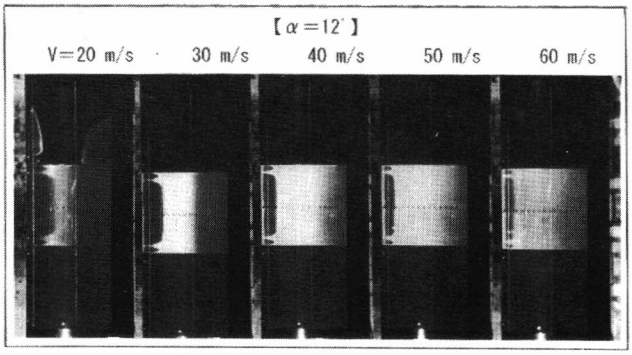

Fig.22 Flow visualization results on NACA 4412

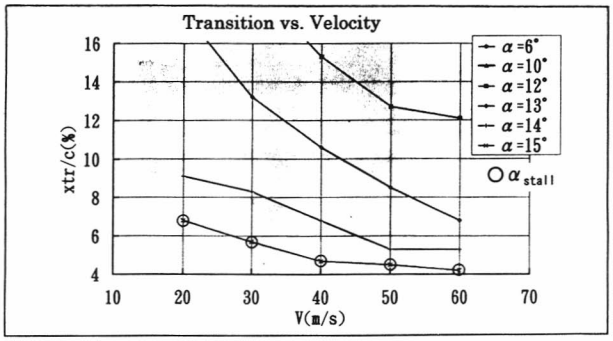

Fig.23 Summary of flow visualization results on NACA 4412 : Transition point vs. Velocity

5. Further Study

In order to advance our study , it is necessary to develop a more detailed criterion than Fig.9 . As a first trial , we continued present numerical analysis for more lots of airfoils in detail . Consequently the behavior of a suction peak , a laminar separation and a transition point could be summarized in four patterns shown in Fig.24 .

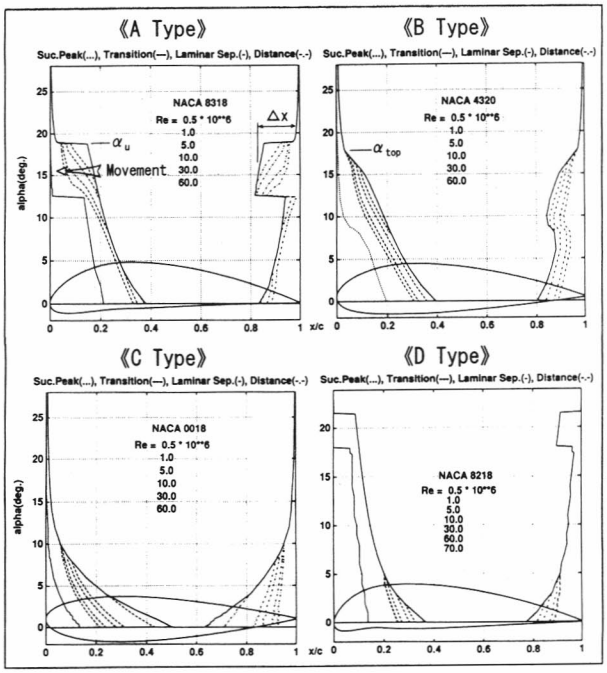

Fig.24 Four typical patterns on the relation between laminar separation and transition

Then we assumed the judgment conditions indicated in the upper part of Fig.25 , based on some experimental results by NACA and our tests . Therefore , a detailed criterion on the adverse effect is summarized as shown in the lower part of

Fig.25 . The ordinate denotes a maximum camber (f/c) and the abscissa shows a thickness ratio (t/c) . This figure means that airfoils with parameters specified by symbols such as △ , ○ , □ and ▽ show the adverse effect . In this figure , these open symbols correspond to the possibility indicated by the symbol of a closed circle (●) in Fig.9 .

It is estimated from this criterion that airfoils with a maximum camber less than 3% or with a thickness ratio less than 12% show no adverse effect . And in airfoils with a maximum camber position x_m/c less than 40% , the boundary showing no adverse effect is extended to the maximum camber of about 5% and the thickness ratio of about 17% .

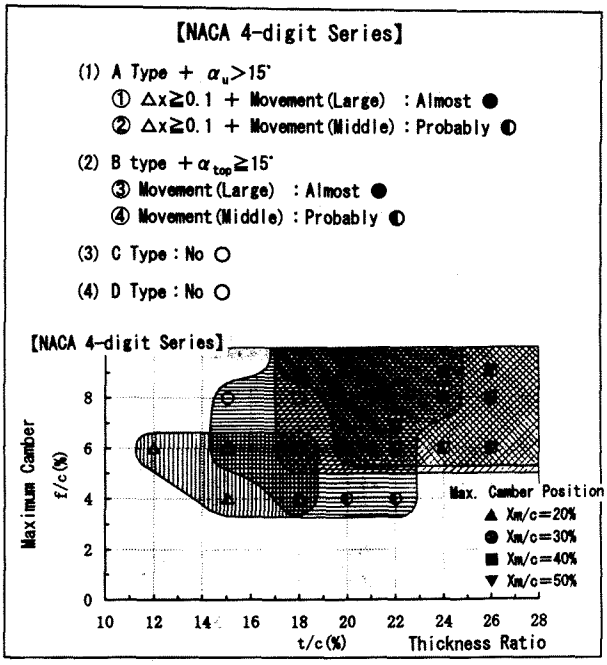

Fig.25 A criterion on the occurrence of adverse effect

We are presently considering that this criterion is approximately useful to judge the occurrence of the adverse effect on the other airfoils as well as NACA 4-digit series airfoils . Because it is supposed that there is no difference between NACA 4-digit series and other airfoils in its mechanism . The boundary is , however , not always clear . In order to develop a complete criterion , therefore , a further study on the other airfoils is desired .

Concluding Remarks

Present numerical and experimental studies for the adverse effect on the C_{lmax} of NACA 4-digit series airfoils made clear that its mechanism explained by Tani was qualitatively valid . Then according to the results obtained by NACA and our test , we proposed a criterion on the occurrence of the adverse effect . Presently we are considering that this is approximately useful to judge whether various airfoils show the adverse effect or not , in spite of being derived on NACA 4-digit series airfoils . In predicting the quantitative behavior on the C_{lmax} at a high Reynolds number , however , a more detailed criterion and further studies are desired .

References

1. Hardy,B.C. : Experimental Investigation of Attachment-Line Transition in Low-Speed , High-Lift Wind Tunnel Testing, AGARD-CP -438, 2-1, 1989
2. Mack,M.D. and McMasters,J.H. : High Reynolds Number Testing in Support of Transonic Airplane Development, AIAA-92 -3982, 1992
3. Jacobs,E.N. and Sherman,A. : Airfoil Section Characteristics as Affected by Variations of the Reynolds Number, NACA Report No.586, 1936
4. Kamiya,N., et al. : Some Practical Aspects of the Burst of Laminar Separation Bubbles, ICAS -80-10.2, 1980
5. Tani, I. : Applied Fluid Dynamics (in Japanese), Iwanami Course, Physics, P.81, 1940
6. Imai,I. : Arbitrary Airfoil Theory (in Japanese), The Journal of the Society of Aeronautical Science of Nippon, Vol.9, No.88, pp.865-875, 1942
7. Thwaite,B. :Approximate calculation of laminar boundary layer, Aero. Quart., Vol.1, pp.245-280, 1949
8. Cebeci,T., et al. : Calculation of Viscous Drag in Incompressible Flows, J. Aircraft, Vol.9, No.10, 1972 .